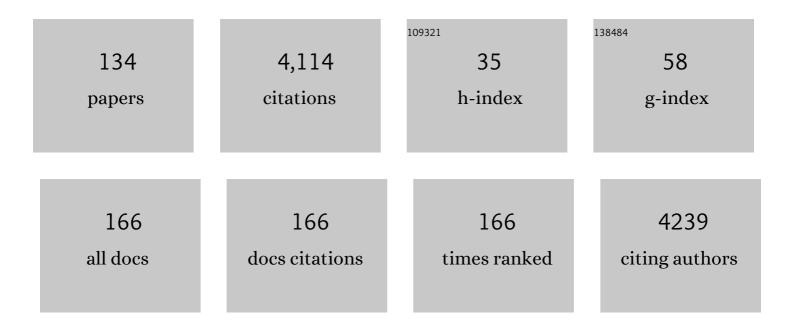
George P Petropoulos

List of Publications by Year in descending order

Source: https://exaly.com/author-pdf/7871147/publications.pdf Version: 2024-02-01



#	Article	IF	CITATIONS
1	Surface soil moisture retrievals from remote sensing: Current status, products & future trends. Physics and Chemistry of the Earth, 2015, 83-84, 36-56.	2.9	320
2	A review of Ts/VI remote sensing based methods for the retrieval of land surface energy fluxes and soil surface moisture. Progress in Physical Geography, 2009, 33, 224-250.	3.2	239
3	Support vector machines and object-based classification for obtaining land-use/cover cartography from Hyperion hyperspectral imagery. Computers and Geosciences, 2012, 41, 99-107.	4.2	189
4	A new synergistic approach for monitoring wetlands using Sentinels -1 and 2 data with object-based machine learning algorithms. Environmental Modelling and Software, 2018, 104, 40-54.	4.5	134
5	Co-Orbital Sentinel 1 and 2 for LULC Mapping with Emphasis on Wetlands in a Mediterranean Setting Based on Machine Learning. Remote Sensing, 2017, 9, 1259.	4.0	125
6	The International Soil Moisture Network: serving Earth system science for over a decade. Hydrology and Earth System Sciences, 2021, 25, 5749-5804.	4.9	116
7	Hyperion hyperspectral imagery analysis combined with machine learning classifiers for land use/cover mapping. Expert Systems With Applications, 2012, 39, 3800-3809.	7.6	104
8	Burnt area delineation from a uni-temporal perspective based on Landsat TM imagery classification using Support Vector Machines. International Journal of Applied Earth Observation and Geoinformation, 2011, 13, 70-80.	2.8	103
9	Towards improved spatio-temporal resolution soil moisture retrievals from the synergy of SMOS and MSG SEVIRI spaceborne observations. Remote Sensing of Environment, 2016, 180, 403-417.	11.0	103
10	A Comparison of Spectral Angle Mapper and Artificial Neural Network Classifiers Combined with Landsat TM Imagery Analysis for Obtaining Burnt Area Mapping. Sensors, 2010, 10, 1967-1985.	3.8	100
11	Land use/land cover in view of earth observation: data sources, input dimensions, and classifiers—a review of the state of the art. Geocarto International, 2021, 36, 957-988.	3.5	89
12	Exploring the relationships between post-fire vegetation regeneration dynamics, topography and burn severity: A case study from the Montane Cordillera Ecozones of Western Canada. Applied Geography, 2015, 56, 232-248.	3.7	83
13	Surface soil moisture retrievals over partially vegetated areas from the synergy of Sentinel-1 and Landsat 8 data using a modified water-cloud model. International Journal of Applied Earth Observation and Geoinformation, 2018, 72, 76-85.	2.8	83
14	Quantifying land use/land cover spatio-temporal landscape pattern dynamics from Hyperion using SVMs classifier and FRAGSTATS [®] . Geocarto International, 2018, 33, 862-878.	3.5	76
15	Erosion rate predictions from PESERA and RUSLE at a Mediterranean site before and after a wildfire: Comparison & implications. Geoderma, 2016, 261, 44-58.	5.1	75
16	Examining the Capability of Supervised Machine Learning Classifiers in Extracting Flooded Areas from Landsat TM Imagery: A Case Study from a Mediterranean Flood. Remote Sensing, 2015, 7, 3372-3399.	4.0	66
17	A global Bayesian sensitivity analysis of the 1d SimSphere soil–vegetation–atmospheric transfer (SVAT) model using Gaussian model emulation. Ecological Modelling, 2009, 220, 2427-2440.	2.5	60
18	Determining the use of Sentinel-2A MSI for wildfire burning & severity detection. International Journal of Remote Sensing, 2019, 40, 905-930.	2.9	60

#	Article	IF	CITATIONS
19	Quantifying spatial and temporal vegetation recovery dynamics following a wildfire event in a Mediterranean landscape using EO data and GIS. Applied Geography, 2014, 50, 120-131.	3.7	57
20	Change detection of surface mining activity and reclamation based on a machine learning approach of multi-temporal Landsat TM imagery. Geocarto International, 2013, 28, 323-342.	3.5	55
21	Remote sensing and GIS analysis for mapping spatio-temporal changes of erosion and deposition of two Mediterranean river deltas: The case of the Axios and Aliakmonas rivers, Greece. International Journal of Applied Earth Observation and Geoinformation, 2015, 35, 217-228.	2.8	53
22	Discrimination of common Mediterranean plant species using field spectroradiometry. International Journal of Applied Earth Observation and Geoinformation, 2011, 13, 922-933.	2.8	50
23	A new method for estimating of evapotranspiration and surface soil moisture from optical and thermal infrared measurements: the simplified triangle. International Journal of Remote Sensing, 2019, 40, 7716-7729.	2.9	50
24	Spectral angle mapper and object-based classification combined with hyperspectral remote sensing imagery for obtaining land use/cover mapping in a Mediterranean region. Geocarto International, 2013, 28, 114-129.	3.5	49
25	Landscape transform and spatial metrics for mapping spatiotemporal land cover dynamics using Earth Observation data-sets. Geocarto International, 0, , 1-15.	3.5	46
26	GIS and Remote Sensing Aided Information for Soil Moisture Estimation: A Comparative Study of Interpolation Techniques. Resources, 2019, 8, 70.	3.5	46
27	WRF Dynamical Downscaling and Bias Correction Schemes for NCEP Estimated Hydro-Meteorological Variables. Water Resources Management, 2015, 29, 2267-2284.	3.9	45
28	Earth Observation-Based Operational Estimation of Soil Moisture and Evapotranspiration for Agricultural Crops in Support of Sustainable Water Management. Sustainability, 2018, 10, 181.	3.2	44
29	Combining ASTER multispectral imagery analysis and support vector machines for rapid and cost-effective post-fire assessment: a case study from the Greek wildland fires of 2007. Natural Hazards and Earth System Sciences, 2010, 10, 305-317.	3.6	43
30	Land cover mapping with emphasis to burnt area delineation using co-orbital ALI and Landsat TM imagery. International Journal of Applied Earth Observation and Geoinformation, 2012, 18, 344-355.	2.8	42
31	Hyperspectral remote sensing in precision agriculture: present status, challenges, and future trends. , 2020, , 121-146.		41
32	Use of Hyperion for Mangrove Forest Carbon Stock Assessment in Bhitarkanika Forest Reserve: A Contribution Towards Blue Carbon Initiative. Remote Sensing, 2020, 12, 597.	4.0	41
33	Spatiotemporal variability of COVID-19 pandemic in relation to air pollution, climate and socioeconomic factors in Pakistan. Chemosphere, 2021, 271, 129584.	8.2	41
34	Heavy Metal Soil Contamination Detection Using Combined Geochemistry and Field Spectroradiometry in the United Kingdom. Sensors, 2019, 19, 762.	3.8	40
35	An Appraisal of the Potential of Landsat 8 in Estimating Chlorophyll-a, Ammonium Concentrations and Other Water Quality Indicators. Remote Sensing, 2018, 10, 1018.	4.0	39
36	Urban vegetation cover extraction from hyperspectral imagery and geographic information system spatial analysis techniques: case of Athens, Greece. Journal of Applied Remote Sensing, 2015, 9, 096088.	1.3	38

#	Article	IF	CITATIONS
37	Soil erosion in future scenario using CMIP5 models and earth observation datasets. Journal of Hydrology, 2021, 594, 125851.	5.4	38
38	Evaluation of diverse classification approaches for land use/cover mapping in a Mediterranean region utilizing Hyperion data. International Journal of Digital Earth, 2014, 7, 194-216.	3.9	37
39	Appraisal of the Sentinel-1 & 2 use in a large-scale wildfire assessment: A case study from Portugal's fires of 2017. Applied Geography, 2018, 100, 78-89.	3.7	36
40	An Overview of the Use of the SimSphere Soil Vegetation Atmosphere Transfer (SVAT) Model for the Study of Land-Atmosphere Interactions. Sensors, 2009, 9, 4286-4308.	3.8	35
41	Exploring the Potential of Sentinels-1 & 2 of the Copernicus Mission in Support of Rapid and Cost-effective Wildfire Assessment. International Journal of Applied Earth Observation and Geoinformation, 2018, 73, 262-276.	2.8	35
42	Drought Identification and Trend Analysis Using Long-Term CHIRPS Satellite Precipitation Product in Bundelkhand, India. Sustainability, 2021, 13, 1042.	3.2	33
43	Flooding extent cartography with Landsat TM imagery and regularized kernel Fisher's discriminant analysis. Computers and Geosciences, 2013, 57, 24-31.	4.2	31
44	An appraisal of the accuracy of operational soil moisture estimates from SMOS MIRAS using validated <i>in situ</i> observations acquired in a Mediterranean environment. International Journal of Remote Sensing, 2014, 35, 5239-5250.	2.9	30
45	Operational evapotranspiration estimates from SEVIRI in support of sustainable water management. International Journal of Applied Earth Observation and Geoinformation, 2016, 49, 175-187.	2.8	29
46	Seasonal evaluation of evapotranspiration fluxes from MODIS satellite and mesoscale model downscaled global reanalysis datasets. Theoretical and Applied Climatology, 2016, 124, 461-473.	2.8	27
47	Geoinformation Technologies in Support of Environmental Hazards Monitoring under Climate Change: An Extensive Review. ISPRS International Journal of Geo-Information, 2021, 10, 94.	2.9	27
48	An Operational In Situ Soil Moisture & Soil Temperature Monitoring Network for West Wales, UK: The WSMN Network. Sensors, 2017, 17, 1481.	3.8	26
49	Investigating connections between COVID-19 pandemic, air pollution and community interventions for Pakistan employing geoinformation technologies. Chemosphere, 2021, 272, 129809.	8.2	25
50	A GIS-based exploration of the relationships between human health, social deprivation and ecosystem services: The case of Wales, UK. Applied Geography, 2013, 45, 77-88.	3.7	24
51	Quantifying Land Cover Changes in a Mediterranean Environment Using Landsat TM and Support Vector Machines. Forests, 2020, 11, 750.	2.1	24
52	Satellite Remote Sensing of Surface Soil Moisture. , 2013, , 85-120.		20
53	Evaluation of the Soil Moisture Operational Estimates From SMOS in Europe: Results Over Diverse Ecosystems. IEEE Sensors Journal, 2015, 15, 5243-5251.	4.7	20
54	Sensitivity analysis of artificial neural network for chlorophyll prediction using hyperspectral data. Environment, Development and Sustainability, 2021, 23, 5504-5519.	5.0	20

GEORGE P PETROPOULOS

#	Article	IF	CITATIONS
55	A sensitivity analysis of the SimSphere SVAT model in the context of EO-based operational products development. Environmental Modelling and Software, 2013, 49, 166-179.	4.5	19
56	Coupling remote sensing with a water balance model for soybean yield predictions over large areas. Earth Science Informatics, 2020, 13, 345-359.	3.2	19
57	Temperature and Humidity Profile Retrieval from FY4-GIIRS Hyperspectral Data Using Artificial Neural Networks. Remote Sensing, 2020, 12, 1872.	4.0	19
58	Addressing the ability of a land biosphere model to predict key biophysical vegetation characterisation parameters with Global Sensitivity Analysis. Environmental Modelling and Software, 2015, 65, 94-107.	4.5	18
59	Assessing the impact of Chinese FY-3/MERSI AOD data assimilation on air quality forecasts: Sand dust events in northeast China. Atmospheric Environment, 2019, 205, 78-89.	4.1	18
60	Performance Assessment of the SEVIRI Evapotranspiration Operational Product: Results Over Diverse Mediterranean Ecosystems. IEEE Sensors Journal, 2015, 15, 3412-3423.	4.7	17
61	Operational Soil Moisture from ASCAT in Support of Water Resources Management. Remote Sensing, 2019, 11, 579.	4.0	17
62	Deriving forest fire probability maps from the fusion of visible/infrared satellite data and geospatial data mining. Modeling Earth Systems and Environment, 2019, 5, 627-643.	3.4	17
63	Evaluating the capabilities of optical/TIR imaging sensing systems for quantifying soil water content. Geocarto International, 2020, 35, 494-511.	3.5	17
64	Spectral Discrimination of Mediterranean Maquis and Phrygana Vegetation: Results From a Case Study in Greece. IEEE Journal of Selected Topics in Applied Earth Observations and Remote Sensing, 2012, 5, 604-616.	4.9	16
65	Surface Soil Moisture Estimation. , 2013, , 29-48.		15
66	An intercomparison of burnt area estimates derived from key operational products: the Greek wildland fires of 2005–2007. Nonlinear Processes in Geophysics, 2013, 20, 397-409.	1.3	15
67	An Integrated GIS-Hydro Modeling Methodology for Surface Runoff Exploitation via Small-Scale Reservoirs. Water (Switzerland), 2020, 12, 3182.	2.7	15
68	Modelling of Greek Lakes Water Quality Using Earth Observation in the Framework of the Water Framework Directive (WFD). Remote Sensing, 2022, 14, 739.	4.0	15
69	Estimating Chlorophyll-a of Inland Water Bodies in Greece Based on Landsat Data. Remote Sensing, 2020, 12, 2087.	4.0	14
70	Future perspectives and challenges in hyperspectral remote sensing. , 2020, , 429-439.		14
71	Appraisal of SMAP Operational Soil Moisture Product from a Global Perspective. Remote Sensing, 2020, 12, 1977.	4.0	14
72	A modernized version of a 1D soil vegetation atmosphere transfer model for improving its future use in land surface interactions studies. Environmental Modelling and Software, 2017, 90, 147-156.	4.5	13

#	Article	IF	CITATIONS
73	Exploring the use of Unmanned Aerial Vehicles (UAVs) with the simplified â€~triangle' technique for soil water content and evaporative fraction retrievals in a Mediterranean setting. International Journal of Remote Sensing, 2021, 42, 1623-1642.	2.9	13
74	Quantifying the Physical Composition of Urban Morphology throughout Wales Based on the Time Series (1989–2011) Analysis of Landsat TM/ETM+ Images and Supporting GIS Data. Remote Sensing, 2014, 6, 11731-11752.	4.0	12
75	Reference Evapotranspiration Retrievals from a Mesoscale Model Based Weather Variables for Soil Moisture Deficit Estimation. Sustainability, 2017, 9, 1971.	3.2	12
76	Evaporative Fluxes and Surface Soil Moisture Retrievals in a Mediterranean Setting from Sentinel-3 and the "Simplified Triangle― Remote Sensing, 2020, 12, 3192.	4.0	12
77	Long-Term Trend Analysis of Precipitation and Extreme Events over Kosi River Basin in India. Water (Switzerland), 2021, 13, 1695.	2.7	12
78	The impact of COVID-19 pandemic on air pollution: a global research framework, challenges, and future perspectives. Environmental Science and Pollution Research, 2022, , 1.	5.3	12
79	Large scale operational soil moisture mapping from passive MW radiometry: SMOS product evaluation in Europe & USA. International Journal of Applied Earth Observation and Geoinformation, 2019, 80, 206-217.	2.8	11
80	Temperature and Humidity Profiles Retrieval in a Plain Area from Fengyun-3D/HIRAS Sensor Using a 1D-VAR Assimilation Scheme. Remote Sensing, 2020, 12, 435.	4.0	11
81	Optimal band characterization in reformation of hyperspectral indices for species diversity estimation. Physics and Chemistry of the Earth, 2022, 126, 103040.	2.9	10
82	Thermal imaging of Nisyros volcano (Aegean Sea) using ASTER data: estimation of radiative heat flux. International Journal of Remote Sensing, 2010, 31, 4033-4047.	2.9	9
83	Extending the Global Sensitivity Analysis of the SimSphere model in the Context of its Future Exploitation by the Scientific Community. Water (Switzerland), 2015, 7, 2101-2141.	2.7	9
84	Assessing the influence of atmospheric and topographic correction and inclusion of SWIR bands in burned scars detection from high-resolution EO imagery: a case study using ASTER. Natural Hazards, 2015, 78, 1609-1628.	3.4	9
85	Forecasting Arabian Sea level rise using exponential smoothing state space models and ARIMA from TOPEX and Jason satellite radar altimeter data. Meteorological Applications, 2016, 23, 633-639.	2.1	9
86	Immediate Changes in Organic Matter and Plant Available Nutrients of Haplic Luvisol Soils Following Different Experimental Burning Intensities in Damak Forest, Hungary. Forests, 2019, 10, 453.	2.1	9
87	An Integrated Spatiotemporal Pattern Analysis Model to Assess and Predict the Degradation of Protected Forest Areas. ISPRS International Journal of Geo-Information, 2020, 9, 530.	2.9	9
88	Pollution characteristics and human health risk assessments of toxic metals and particle pollutants via soil and air using geoinformation in urbanized city of Pakistan. Environmental Science and Pollution Research, 2021, 28, 58206-58220.	5.3	9
89	A comparative analysis of emulators for the sensitivity analysis of a land surface process model. Procedia, Social and Behavioral Sciences, 2010, 2, 7716-7717.	0.5	8
90	Identification of Painted Rock-Shelter Sites Using GIS Integrated with a Decision Support System and Fuzzy Logic. ISPRS International Journal of Geo-Information, 2018, 7, 326.	2.9	8

#	Article	IF	CITATIONS
91	Mapping and monitoring of the land use/cover changes in the wider area of Itanos, Crete, using very high resolution EO imagery with specific interest in archaeological sites. Environment, Development and Sustainability, 2020, 22, 3433-3460.	5.0	8
92	Microwave Land Emissivity Calculations over the Qinghai-Tibetan Plateau Using FY-3B/MWRI Measurements. Remote Sensing, 2019, 11, 2206.	4.0	7
93	Sensitivity Exploration of SimSphere Land Surface Model Towards Its Use for Operational Products Development from Earth Observation Data. Society of Earth Scientists Series, 2014, , 35-56.	0.3	7
94	Spectroradiometry as a tool for monitoring soil contamination by heavy metals in a floodplain site. , 2020, , 249-268.		7
95	Identifying Spatially Correlated Patterns between Surface Water and Frost Risk Using EO Data and Geospatial Indices. Water (Switzerland), 2020, 12, 700.	2.7	6
96	The Use of Hyperspectral Earth Observation Data for Land Use/Cover ClassificationPresent Status, Challenges, and Future Outlook. , 2018, , 147-173.		6
97	Exploring the potential of SCAT-SAR SWI for soil moisture retrievals at selected COSMOS-UK sites. International Journal of Remote Sensing, 2021, 42, 9155-9169.	2.9	6
98	Tree's detection & health's assessment from ultra-high resolution UAV imagery and deep learning. Geocarto International, 2022, 37, 10459-10479.	3.5	6
99	A decision support system-based procedure for evaluation and monitoring of protected areas sustainability for the Mediterranean region. Journal of Earth System Science, 2011, 120, 949-961.	1.3	5
100	Turbulent Fluxes of Heat and Moisture at the Earthâ \in ™s Land Surface. , 2013, , 3-28.		5
101	Remote Sensing of Surface Turbulent Energy Fluxes. , 2013, , 49-84.		5
102	Quantifying the prediction accuracy of a 1-D SVAT model at a range of ecosystems in the USA and Australia: evidence towards its use as a tool to study Earth's system interactions. Geoscientific Model Development, 2015, 8, 3257-3284.	3.6	5
103	Detection and Analysis of C-Band Radio Frequency Interference in AMSR2 Data over Land. Remote Sensing, 2019, 11, 1228.	4.0	5
104	Band selection algorithms for foliar trait retrieval using AVIRIS-NG: a comparison of feature based attribute evaluators. Geocarto International, 2022, 37, 4071-4087.	3.5	5
105	Temperature and Relative Humidity Profile Retrieval from Fengyun-3D/HIRAS in the Arctic Region. Remote Sensing, 2021, 13, 1884.	4.0	5
106	Random Forests with Bagging and Genetic Algorithms Coupled with Least Trimmed Squares Regression for Soil Moisture Deficit Using SMOS Satellite Soil Moisture. ISPRS International Journal of Geo-Information, 2021, 10, 507.	2.9	5
107	Seasonal Trends in Clouds and Radiation over the Arctic Seas from Satellite Observations during 1982 to 2019. Remote Sensing, 2021, 13, 3201.	4.0	5
108	Reduced major axis approach for correcting GPM/GMI radiometric biases to coincide with radiative transfer simulation. Journal of Quantitative Spectroscopy and Radiative Transfer, 2016, 168, 40-45.	2.3	4

#	Article	IF	CITATIONS
109	Variational Bayes and the Principal Component Analysis Coupled With Bayesian Regulation Backpropagation Network to Retrieve Total Precipitable Water (TPW) From GCOM-W1/AMSR2. IEEE Journal of Selected Topics in Applied Earth Observations and Remote Sensing, 2015, 8, 4819-4824.	4.9	3
110	Soil Moisture Deficit Estimation Through SMOS Soil Moisture and MODIS Land Surface Temperature. , 2016, , 333-347.		3
111	Uncertainty Quantification in the Infrared Surface Emissivity Model (ISEM). IEEE Journal of Selected Topics in Applied Earth Observations and Remote Sensing, 2016, 9, 5888-5892.	4.9	3
112	GEM-SA., 2017,, 341-361.		3
113	SMAP Soil Moisture Product Assessment over Wales, U.K., Using Observations from the WSMN Ground Monitoring Network. Sustainability, 2021, 13, 6019.	3.2	3
114	EXPLORING THE POTENTIAL OF EO DATA AND GIS FOR ECOSYSTEM HEALTH MODELING IN RESPONSE TO WILDFIRE: A CASE STUDY IN CENTRAL GREECE. Environmental Engineering and Management Journal, 2018, 17, 2165-2178.	0.6	3
115	Statistical Unfolding Approach to Understand Influencing Factors for Taxol Content Variation in High Altitude Himalayan Region. Forests, 2021, 12, 1726.	2.1	3
116	Satellite radiance assimilation using a 3DVAR assimilation system for hurricane Sandy forecasts. Natural Hazards, 2016, 82, 845-855.	3.4	2
117	SEVIRI PrePro: A novel software tool for the pre-processing of SEVIRI geostationary orbit EO data products. Environmental Modelling and Software, 2016, 82, 321-329.	4.5	2
118	Retrievals of key biophysical parameters at mesoscale from the Ts/VI scatterplot domain. Geocarto International, 2020, , 1-21.	3.5	2
119	Cross-Validation of Radio-Frequency-Interference Signature in Satellite Microwave Radiometer Observations over the Ocean. Remote Sensing, 2020, 12, 3433.	4.0	2
120	Future pathway for research and emerging applications in GPS/GNSS. , 2021, , 429-438.		2
121	Synergistic Evaluation of Passive Microwave and Optical/IR Data for Modelling Vegetation Transmissivity towards Improved Soil Moisture Retrieval. Sensors, 2022, 22, 1354.	3.8	2
122	A decision support system for assessing and managing environment risk cross borders. Earth Science Informatics, 2011, 4, 107-115.	3.2	1
123	Land Use Cartography from Hyperion Hyperspectral Imagery Analysis: Results from a Mediterranean Site. , 2012, , .		1
124	Synthesis and characterization of 5-amino-1,3,6-trinitro-1H-benzo[d]imidazol-2(3H)-one as an energetic material. RSC Advances, 2014, 4, 42215-42219.	3.6	1
125	Spatiotemporal Estimates of Surface Soil Moisture from Space Using the Ts/VI Feature Space. , 2016, , 91-108.		1
126	Exploring the synergy between Landsat and ASAR towards improving thematic mapping accuracy of optical EO data. Applied Geomatics, 2019, 11, 277-288.	2.5	1

#	Article	IF	CITATIONS
127	Seasonal variation of key environmental parameters in the Sea of Oman using EO data and GIS. Environment, Development and Sustainability, 2021, 23, 6021-6046.	5.0	1
128	Special Section Guest Editorial: Recent Advances in Earth Observation Technologies for Agrometeorology and Agroclimatology. Journal of Applied Remote Sensing, 2018, 12, 1.	1.3	1
129	Overview of Sensitivity Analysis Methods in Earth Observation Modeling. , 2017, , 3-24.		0
130	A Two-Season Impact Study of Radiative Forced Tropospheric Response to Stratospheric Initial Conditions Inferred From Satellite Radiance Assimilation. Climate, 2019, 7, 114.	2.8	0
131	Modelling key parameters characterising land surface using the SimSphere SVAT model. , 2021, , 409-442.		0
132	A preliminary evaluation of the †̃simplified triangle' with Sentinel-3 images for mapping surface soil moisture and evaporative fluxes. , 2021, , 209-223.		0
133	PROgRESSIon—Investigating the Prototyping of Operational Estimation of Energy Fluxes and Soil Moisture Content Using a Variant of the "Triangle―Inversion Methodology. Springer Earth System Sciences, 2016, , 107-125.	0.2	0
134	Investigation of the Sensitivity of Microwave Land Surface Emissivity to Soil Texture in MLEM. Remote Sensing, 2022, 14, 3045.	4.0	0